Vehicular Communication Networks with Platooned Vehicles: Modeling and Analysis

Kaushlendra Pandey, Abhishek K. Gupta, Kanaka Raju Perumalla, Harpreet S. Dhillon

Abstract—**Vehicular platooning is a promising solution to increase road capacity and ensure a seamless traffic flow. Despite its relevance in the current vehicular networks, its rigorous system-level analysis has not been performed yet. In this work, we develop a comprehensive framework to model and analyze a vehicular communication network with platooned traffic. The network of roads is modeled as a Poisson line process (PLP) and vehicles are placed on each road according to an independent Matérn cluster process (MCP) to capture platooning. The resulting point process formed by the locations of the vehicles is a Cox process driven by a PLP, which we term as the PLP-MCP. We first characterize PLP-MCP and present some of its key properties. Assuming that the cellular BSs are distributed as an independent Poisson point process (PPP), we then derive the load distribution on the typical BS of the network which is an important ingredient in the analysis of many key performance metrics, such as coverage probability and the rate distribution over the network. We then provide several system-design insights, including the impact of platooning on coverage probability.**

I. Introduction

Vehicle platooning is the coordinated movement of a group of vehicles traveling over a common route or a segment of it. Platooning as a component of intelligent transportation systems offers many benefits including preventing vehicle collisions, optimizing road capacity and fuel consumption, and lowering the emission of pollutants [2]. Platoon formation and vehicular communications are intertwined. On one hand, platooning facilitates line-of-sight communication between two proximate vehicles, thereby improving vehicle-to-vehicle (V2V) communication between them in comparison to independently moving vehicles [3]. Additionally, V2V communication may assist broadcast information to all vehicles in the platoon if one vehicle in the platoon is able to receive it through vehicle-to-infrastructure (V2I) communication. On the other hand, vehicular communication also facilitates platooning by reducing collision risks. Given the interdependent nature of these two seemingly unrelated concepts, it is crucial to understand their interplay, which we achieve by incorporating platooning into a system-level study of vehicular networks.

Related work: The system-level analysis of vehicular communication networks using stochastic geometry has attracted considerable interest in recent years [4]–[11]. However, the focus of the most of the prior work has been on conventional *non-platooning traffic scenarios* (N-PTS), where vehicles move in uncoordinated fashion without forming any platoons. For instance, to incorporate multi-road vehicular traffic in the analysis, in [4], authors suggested to model roads as PLP and vehicles on each road as a 1D PPP. In this model, the combined vehicular traffic across roads forms a Cox process termed as PLP-PPP (*i.e.* a PLP driven PPP). In [5] authors presented the Laplace functional (LF) of the PLP-PPP and using the LF authors derived the nearest neighbor distance distribution of PLP-PPP. In [6], authors derived the typical user's coverage probability when cellular and vehicular BSs are modeled as 2D PPP and PLP-PPP, respectively. A thorough investigation of various properties of PLP-PPP and its applications to vehicular communications was recently presented in [7].

A vehicular communication network consists of vehicular traffic overlaid with a cellular network to provide infrastructure connectivity to vehicular traffic. Such a network with N-PTS can be modeled using PLP-PPP on top of a separate PPP that models the locations of BSs. In [8], authors derived the distribution of signal-to-noise-plus-interference ratio (SINR) for similar models. In [9], authors derived the distribution of the per-BS load and per-user rate for N-PTS. Although past works have analyzed the vehicular communication network with N-PTS, analytical tools have not been fully explored yet to study the *platooned vehicular traffic scenario* (PTS) and its impact on the performance of a vehicular communication network. Consequently, there is a limited work focusing on the analysis of PTS [10], [11]. For example, in [10] authors considered vehicular traffic composed of vehicles moving independently on a road. Each vehicle can communicate with vehicles lying within a specific transmission range. The authors derive the connectivity probability, which is defined as the probability that the inter-vehicle distance between every vehicle is less than the vehicle's transmission range. In [11], authors derived coverage probability for a setting consisting of platooned traffic on a single road with BSs deployed on the side of the same road. One main limitation of all these works focusing on vehicular platooning is that they considered vehicular traffic on a single road. In practice, the "support" of a vehicular network is a complicated layout of roads that needs to be accounted for and is one of the key reasons for the popularity of the PLP-based models. Since the system-level performance of any wireless network critically depends upon the topology of its nodes, it is crucial to include platooning in the state-of-the-art PLP-based spatial models and develop corresponding mathematical tools for analysis and design, which is the main goal of this paper.

Contributions: In this paper, we develop an analytical frame-

K. Pandey, A. K. Gupta and K. Raju Perumalla are with IIT Kanpur, India, 208016. Email:{kpandey,gkrabhi,pkraju}@iitk.ac.in. H. S. Dhillon is with Wireless@VT, Virginia Tech, Blacksburg, VA 24061 (Email: hdhillon@vt.edu). The extended version of this work is submitted to IEEE Trans. Wireless Commun. [1]. H. S. Dhillon gratefully acknowledges the support of the US National Science Foundation (Grant CNS-1923807).

work for a V2I communication system with platooned traffic. We propose a novel point process (PP) termed PLP-MCP for the modeling and analysis of the platooned movement of the vehicles on a system of roads. It is a Cox process driven by the PLP that captures three layers of randomness: (i) irregularity in the road layout, (ii) randomness in the locations of the platoons, and (iii) randomness in the locations of vehicles within a platoon. In this sense, this process can be thought of as a *triply-stochastic* process that generalizes *doubly-stochastic* PLP-PPP used in the literature [7]. We then consider a communication network consisting of BSs overlaid on the platoon traffic and compute the load distribution on the typical BS. The load distribution acts as an important performance metric as it critically affects the distribution of SINR, per-user available resources, and the rate.

Notation: Vectors in $\mathbb{R}$ are denoted by bold *italic* style letters (*e.g.* $\boldsymbol{x}$) with their norms as $|\boldsymbol{x}|$. Similarly, vectors in $\mathbb{R}^2$ are denoted by bold style letters (*e.g.* $\mathbf{x}$) with their norms as $\|\mathbf{x}\|$. The origin is $\mathrm{o} \equiv (0,0)$. Let $\mathsf{B}_1(\boldsymbol{x}, r)$ and $\mathsf{B}_2(\mathbf{x}, r)$ denote a 1D and 2D ball centered at $\boldsymbol{x}$ and $\mathbf{x}$ respectively of radius r. Let $\ell = \mathsf{L}(\rho, \phi)$ denotes a line in $\mathbb{R}^2$ in Hesse normal form, *i.e.* the normal segment from origin to the line is of length ρ and makes angle ϕ with respect to the x-axis. The point $(\rho\cos\phi, \rho\sin\phi)$ is the nearest point on the line $\mathsf{L}(\rho, \phi)$ from the origin termed the base. The line $\mathsf{L}(\rho, \phi)$ can also be represented as an element (ρ, ϕ) of the set $\mathbf{C}^* \equiv \mathbb{R} \times [0, \pi)$. We term the element (ρ, ϕ) as L-atom (line atom) and $\mathbf{C}^*$ as L-space. Further, $f_\ell(\cdot)$ denotes the transformation of $\mathsf{L}(0,0)$ to the line $\ell = \mathsf{L}(\rho_\ell, \phi_\ell)$ given as

$$f_\ell(\overline{\boldsymbol{x}}) = (\rho_\ell \cos\phi_\ell + \overline{\boldsymbol{x}}\sin\phi_\ell, \rho_\ell\sin\phi_\ell - \overline{\boldsymbol{x}}\cos\phi_\ell). \quad (1)$$

This means that if $\overline{\boldsymbol{x}}$ is a scalar quantity denoting the location of a point in the line ℓ relative to its base, its 2D coordinates (*i.e.* absolute location in $\mathbb{R}^2$) are given as $\mathbf{x} = f_\ell(\overline{\boldsymbol{x}})$. For a set A, $|\mathsf{A}|$ denotes its Lebesgue measure in its respective dimension, for example $|\mathsf{B}_1(\mathrm{o}, r)| = 2r$. The PDF of the generalized Gamma distribution with parameters a_1, b_1, c_1 is denoted by

$$\tilde{g}_X(x; a_1, b_1, c_1) = \frac{a_1 b_1^{c_1/a_1}}{\Gamma(c_1/a_1)} x^{c_1-1} e^{-b_1 x^{a_1}}. \quad (2)$$

For a PP Ψ, the notation $\Psi(\mathsf{C})$ denotes the number of points of Ψ falling inside set C. The PGF of any integer-valued random variable (RV) X is denoted by $\mathcal{P}_X(\cdot)$. The expected value of RV X is denoted by $\mathbb{E}[X]$ and $\beta(r) = 2\min(r, a)$.

II. Modeling of Platooned Vehicles using PLP-MCP

In this paper, we consider a vehicular traffic with platooned vehicles on a system on roads as well as a cellular network to provide connectivity. The system model is described next.

A. Road network

We considered that roads are distributed as PLP $\Phi_{\mathrm{L}} = \{\ell_1, \ell_2, \cdots\}$ with density λ_{L} where ℓ_i denotes the i-th road [7]. The i-th line $\ell_i \in \Phi_{\mathrm{L}}$ can be denoted by the L-atom $a_i = (\rho_{\ell_i}, \phi_{\ell_i})$ in the L-space $\mathbf{C}^*$. The L-atoms a_i's form a PPP in $\mathbf{C}^*$ with density λ_{L}. This means that the mean number of lines hitting a convex body K with perimeter $L(\mathsf{K})$ is $\lambda_{\mathrm{L}} L(\mathsf{K})$ [7].

B. Platooned vehicles

For each road ℓ_i, vehicular platoons can be seen as the clusters of vehicles in a finite spread. Since the vehicles are usually uniformly distributed in the respective platoons, it is natural to model the resulting traffic on each road using MCPs. We model the vehicles on the road ℓ_i by an independent MCP Ψ_i with parent PP density λ_{P}, mean number of points per cluster m and cluster radius a. In particular, the platoon centers are distributed as the parent PP $\overline{\Psi}_i^{(\mathrm{p})}$. For a platoon centered at $\boldsymbol{x}_{j,i} \in \overline{\Psi}_i^{(\mathrm{p})}$, the constituent vehicles are distributed as the PPP $\overline{\Omega}_{\boldsymbol{x}_{j,i}}$ in $a-$neighborhood of it. Let μ_{m} denote the per-road vehicular density *i.e.* $\mu_{\mathrm{m}} = m\lambda_{\mathrm{P}}$.

The locations of all vehicles form a novel PP, which we introduce in this paper and term as PLP-MCP. It can be formally defined as follows.

Definition 1 (PLP-MCP). *Let $\Phi_{\mathrm{L}} = \{\ell_1, \ell_2, \cdots\}$ be a PLP with density λ_{L} with the i-th line $\ell_i = \mathsf{L}(\rho_{\ell_i}, \phi_{\ell_i})$. Let $\{\overline{\Psi}_i\}$ be a set of independent and identically distributed 1D MCP in $\mathbb{R}$ with parameter $(m, \lambda_{\mathrm{P}}, a)$ such that*

$$\overline{\Psi}_i = \bigcup\nolimits_{\boldsymbol{x}_{j,i} \in \overline{\Psi}_i^{(\mathrm{p})}} \overline{\Omega}_{\boldsymbol{x}_{j,i}},$$

where $\overline{\Psi}_i^{(\mathrm{p})}$ is a PPP with density λ_{P}. Here, $\overline{\Psi}_i^{(\mathrm{p})}$ is called the parent PP of $\overline{\Psi}_i$ as it consists of parent points $\boldsymbol{x}_{j,i} \in \mathbb{R}$. Further, $\overline{\Omega}_{\boldsymbol{x}_{j,i}}$ denotes the daughter PP of $\boldsymbol{x}_{j,i}$ and is a PPP with density $\lambda_{\mathrm{d}} = m/(2a)$ in $\mathsf{B}_1(\boldsymbol{x}_{j,i}, a)$. We assign i-th MCP $\overline{\Psi}_i$ to the i-th line ℓ_i and transform the points of $\overline{\Psi}_i$ to be on the line to get

$$\Psi_{\ell_i} = \bigcup\nolimits_{\boldsymbol{x}_{j,i} \in \overline{\Psi}_i^{(\mathrm{p})}} \{\mathbf{z}_{k,j,i} = f_{\ell_i}(\overline{\boldsymbol{z}}_{k,j,i}) : \overline{\boldsymbol{z}}_{k,j,i} \in \overline{\Omega}_{\boldsymbol{x}_{j,i}}\}$$
$$= \bigcup\nolimits_{\boldsymbol{x}_{j,i} \in \overline{\Psi}_i^{(\mathrm{p})}} \Omega_{\boldsymbol{x}_{j,i}}, \quad (3)$$

where $\Omega_{\boldsymbol{x}_{j,i}}$ represents $\overline{\Omega}_{\boldsymbol{x}_{j,i}}$ transformed on line ℓ_i. Now, a PLP-MCP Ψ_{m} is defined as the union of all Ψ_{ℓ_i}'s i.e

$$\Psi_{\mathrm{m}} = \bigcup\nolimits_{\ell_i \in \Phi_{\mathrm{L}}} \Psi_{\ell_i}, \quad (4)$$

and includes all the points located on every line of Φ_{L}. Further, the density of the Ψ_{m} is $\lambda_{\mathrm{m}} = m\lambda_{\mathrm{P}}\lambda_{\mathrm{L}}\pi = \mu_{\mathrm{m}}\lambda_{\mathrm{L}}\pi$.

In summary, the platoon vehicular traffic is modeled in this paper using points of the proposed PLP-MCP Ψ_{m}. The absolute location of k-th vehicles in jth platoon of i-th road is given as $\mathbf{z}_{k,j,i}$.

C. Vehicular communication network

A vehicular communication network consists of the vehicular traffic overlaid with the BSs to provide cellular V2I connectivity to vehicular users. We model the locations of BSs as a 2D PPP $\Phi_{\mathrm{b}} \equiv \{\mathbf{y}_i\}$ with density λ_{b} [12]. Each BS transmits with the same power. The user association is based on the maximum average received power from the BSs and each user is connected to its nearest BS. Hence serving region of each BS is its Voronoi cell. The users connected to a BS constitute the load on that BS. Let the typical Voronoi cell be V_t. Its area $|\mathsf{V}_\mathrm{t}|$ is empirically distributed as a generalized Gamma RV [13] with parameters $a_1 = 1.07950, b_1 = 3.03226$ and $c_1 = 3.31122$ [14], *i.e.* its PDF is

$$g_{|\mathsf{V}_\mathrm{t}|}(v_\mathrm{t}) = \lambda_\mathrm{b}\tilde{g}_X\left(\lambda_\mathrm{b}v_\mathrm{t}; a_1, b_1, c_1\right). \quad (5)$$

The *typical point* of the PLP-MCP Ψ_m denotes *the typical vehicle* [12].

III. CHARACTERIZATION OF PLP-MCP

Since PLP-MCP is the key to modeling the platooned vehicles, we will present several key properties of the proposed PLP-MCP to understand this better.

A. Probability generating functional (PGFL) of Ψ_m

To characterize the distribution of PLP-MCP, we now derive its PGFL. For this we require the PGFL of the MCP Ψ_{ℓ_i} transformed on the line ℓ_i which is stated in Lemma 1.

Lemma 1. *Let there be a function $v : \mathbb{R}^2 \to [0, 1]$. The PGFL of Ψ_ℓ on road ℓ is given as [1]*

$$G_{\Psi_\ell,\ell}(v) = \exp\left(-\lambda_\mathrm{P}\int_{\mathbb{R}}\left(1 - \mathcal{H}_{\boldsymbol{x},\ell}(v)\right)\mathrm{d}\boldsymbol{x}\right), \quad (6)$$

where $\mathcal{H}_{\boldsymbol{x},\ell}(v)$ is

$$= \exp\left(-\lambda_\mathrm{d}\int_{\mathsf{B}_1(\mathrm{o},a)}\left(1 - \left(v \circ f_\ell\right)(\boldsymbol{x}+\boldsymbol{y})\right)\mathrm{d}\boldsymbol{y}\right).$$

Now, using the Lemma 1, we derive the PGFL for PLP-MCP.

Theorem 1. *The PGFL for Ψ_m is given as (for proof see Appendix A)*

$$G_{\Psi_\mathrm{m}}(v) = \mathbb{E}\left[\prod_{\mathbf{z}_i\in\Psi_\mathrm{m}} v(\mathbf{z}_i)\right]$$
$$= \exp\left(-\lambda_\mathrm{L}\int_{\mathbb{R}}\int_0^{\pi}\left(1 - G_{\Psi_{\mathsf{L}(\rho,\phi)},\mathsf{L}(\rho,\phi)}(v)\right)\mathrm{d}\rho\,\mathrm{d}\phi\right), \quad (7)$$

where $G_{\Psi_\ell,\ell}(v)$ is given in (6).

Using the PGFL of a PP, we can easily derive some of the key properties of that PP, such as its contact distance (CD) distribution. It is also useful in studying the interference characteristics of the wireless networks modeled using that PP [12].

B. Distribution of number of points (vehicles) of Ψ_m in a 2D ball

Another key property of the PPP Ψ_m is the distribution of the number of its points in a ball, which is crucial in computing the distance distribution of the nearest vehicle from the typical BS and the load distribution in vehicular communication network which will be discussed in the next section. To derive this distribution, we will first require the PGF of the number N_ℓ of points of the MCP Ψ_ℓ on the line ℓ which is given in Lemma 2.

Lemma 2. *Let Ψ_ℓ denotes a 1D MCP on line $\ell = \mathsf{L}(\rho,\phi)$. The PGF for the number N_ℓ of points of Ψ_ℓ falling inside $\mathsf{B}_2(\mathrm{o}, r)$ is*

$$\mathcal{P}_{N_\ell}(s,r) = e^{\left(g(s,\sqrt{r^2-\rho^2})\right)}, \quad (8)$$
$$\textit{where } g(s,t) = 2\lambda_\mathrm{P}\left[|t-a|\,e^{\lambda_\mathrm{d}\beta(t)(s-1)} - (t+a)\right.$$
$$\left. + (e^{\lambda_\mathrm{d}(s-1)\beta(t)} - 1)/(\lambda_\mathrm{d}(s-1))\right]. \quad (9)$$

Note that $\rho = 0$ gives the PGF of N_ℓ when the line passes through the origin with an angle of ϕ. Later in this paper, we will require the k-th derivatives $g^{(k)}(s,t)$ of $g(s,t)$ with respect to s which are given as $g^{(k)}(s,t) =$

$$2\lambda_\mathrm{P}\left[(\lambda_\mathrm{d}\beta(t))^k|t-a|e^{(s-1)\lambda_\mathrm{d}\beta(t)} + \frac{1}{\lambda_\mathrm{d}}\left(\sum_{j=0}^{k}\binom{k}{j}\right.\right.$$
$$\left.\left.\frac{j!(-1)^j}{(s-1)^{j+1}}(\lambda_\mathrm{d}\beta(t))^{k-j}e^{(s-1)\lambda_\mathrm{d}\beta(t)} - \frac{k!(-1)^k}{(s-1)^{k+1}}\right)\right]. \quad (10)$$

We now present the distribution of the number $S(r)$ of points of Ψ_m in a 2D ball of radius r, *i.e.* $S(r) = \Psi_\mathrm{m}(\mathsf{B}_2(\mathrm{o}, r))$ in terms of its PGF. Note that the PMF and the mean of a discrete RV X can be computed easily from its PGF using the following relation

$$p_X(k) \triangleq \mathbb{P}[X = k] = \frac{1}{k!}\left[\mathcal{P}_X^{(k)}(s,r)\right]_{s=0} \quad \forall k, \quad (11)$$
$$\mathbb{E}[X] = \left[\mathcal{P}_X^{(1)}(s)\right]_{s=1}. \quad (12)$$

Theorem 2. *The PGF of the number $S(r)$ of points of Ψ_m inside $\mathsf{B}_2(\mathrm{o}, r)$ is (for proof see Appendix B)*

$$\mathcal{P}_{S(r)}(s) = \exp\left(-2\pi\lambda_\mathrm{L}\left(r - \int_0^r\frac{\exp(g(s,t))t}{\sqrt{r^2-t^2}}\mathrm{d}t\right)\right), \quad (13)$$

where $g(s,t)$ is given in (9).

Using (11) (12), we get the following results.

Corollary 2.1. *The PMF of $S(r)$ is given by*

$$\mathbb{P}[S(r) = n] = \frac{1}{n!}\mathcal{P}_{S(r)}(0)\ \mathsf{b}\left(f_\mathrm{m}^{(1)}(r), \cdots, f_\mathrm{m}^{(n)}(r)\right), \quad (14)$$
$$\textit{with} \quad f_\mathrm{m}^{(k)}(r)$$
$$= 2\pi\lambda_\mathrm{L}\int_0^r\frac{\exp\left(g(0,t)\right)}{\sqrt{r^2-t^2}}\mathsf{b}\left(g^{(1)}(0,t), \cdots, g^{(k)}(0,t)\right)t\mathrm{d}t, \quad (15)$$

where $\mathsf{b}(\cdot)$ denotes the Bell's polynomial [15] and $g^{(k)}(0,t)$ can be evaluated from (10)*. Further, the mean of $S(r)$ is $\mathbb{E}[S(r)] = \lambda_\mathrm{m}\pi r^2$.*

C. CD of PLP-MCP

The k-th CD of a PP is defined as the distance of the k-th closest point of the PP from the origin. Since its CDF is related to the PMF of $S(r)$ as

$$F_{R_k}(r) = \mathbb{P}[R_k \leq r] = \mathbb{P}\left[S(r) \geq k\right],$$

we can get the following result.

Corollary 2.2. *The CDF of the k-th CD of $\Psi_{\rm m}$ is*

$$F_{R_k}(r) = 1 - \sum_{m=0}^{k-1} \frac{1}{m!}\mathcal{P}_{S(r)}(0)\ \mathsf{b}\left(f_{\rm m}^{(1)}(r), \cdots, f_{\rm m}^{(m)}(r)\right).$$

IV. Performance of the Typical BS in a Platooned Vehicular Communication Network

In this section, we present the per-BS load distribution and the SIR coverage of the typical user.

A. Distribution of load on the typical BS

Note that the per-BS load $S_{\rm m}$ in a communication system refers to the number of vehicles served by the typical BS and is equal to the number of users (vehicles) falling inside its serving Voronoi region. Mathematically, $S_{\rm m} = \Psi_{\rm m}(\mathsf{V}_{\rm t})$.

The distribution of per-BS load is an important performance metric as it critically affects the distribution of SINR, per-user available resources and finally the rate in the following way. If a particular BS does not have any user associated with it, it may stay silent which reduces interference to the users of other BSs, and improves their SINR distribution. The load distribution may help us decide the size of platoon and/or the number of vehicles in a platoon to improve performance. It may also provide insights into the load distribution across the BSs that may help in optimizing the resource allocation, bandwidth sharing, and BS association. This is especially important in the case of PTS that may exhibit larger disparity in the per-BS load, especially for smaller values of a. Since vehicles in a platoon drive in close proximity of each other, it is highly likely that vehicles in a given platoon are served by the same BS. This may lead to situations in which one BS serves multiple platoons and hence a large number of vehicles, whereas another BS does not serve any platoon and hence no vehicle. Therefore, it is crucial to understand the nature of load distribution on BSs.

We will look at an approximation ($\widetilde{S}_{\rm m}$) of the load distribution on the typical cell. To approximate the load in a Voronoi cell of area $|V_{\rm t}|$, we will replace the cell with a 2D ball of equal area, *i.e.* the radius of this ball is $R_{\rm t} = \sqrt{|V_{\rm t}|/\pi}$ and instead compute the load in this ball. The PDF of $R_{\rm t}$ is

$$f_{R_{\rm t}}(r_{\rm t}) = 2\pi r_{\rm t} g_{|\mathsf{V}_{\rm t}|}(\pi r_{\rm t}^2). \quad (16)$$

Hence, we can approximate $S_{\rm m}$ by $\widetilde{S}_{\rm m} = \Psi_{\rm m}(\mathsf{B}_2(\mathrm{o}, R_{\rm t}))$. Note that conditioned on $R_{\rm t}$, $\mathcal{P}_{\widetilde{S}_{\rm m}(R_{\rm t})|R_{\rm t}=r_{\rm t}}(s) = \mathcal{P}_{S(r_{\rm t})}(s)$. Deconditioning using the distribution of $f_{R_{\rm t}}(r_{\rm t})$, we get the following result.

Theorem 3. *The approximate PGF and PMF of the typical BS load are*

$$\mathcal{P}_{\widetilde{S}_{\rm m}}(s) = \int_{r_{\rm t}=0}^{\infty} \mathcal{P}_{S(r_{\rm t})}(s)\, f_{R_{\rm t}}(r_{\rm t}){\rm d}r_{\rm t}$$
$$= 2\pi \int_{r_{\rm t}=0}^{\infty} \mathcal{P}_{S(r_{\rm t})}(s)\, r_{\rm t} g_{|V_{\rm t}|}(\pi r_{\rm t}^2){\rm d}r_{\rm t}. \quad (17)$$

$$\mathbb{P}[\widetilde{S}_{\rm m} = k] = 2\pi \int_{r_{\rm t}=0}^{\infty} \mathbb{P}\left[S(r_{\rm t}) = k\right] r_{\rm t} g_{|V_{\rm t}|}(\pi r_{\rm t}^2){\rm d}r_{\rm t}, \quad (18)$$

where $\mathcal{P}_{S(\cdot)}(\cdot)$, and $\mathbb{P}\left[S(r_{\rm t}) = k\right]$ are given in Theorem 2 and (14)*, respectively. The PDF $g_{|V_{\rm t}|}(\cdot)$ is given in* (5).

Corollary 3.1. *The mean of $\widetilde{S}_{\rm m}$ is $\mathbb{E}[\widetilde{S}_{\rm m}] = \lambda_{\rm m}\pi\mathbb{E}\left[r_{\rm t}^2\right] = \lambda_{\rm m}/\lambda_{\rm b}$.*

If a particular BS does not have any users associated with it, it may stay silent to improve coverage. The probability that a BS is active which is termed *active* or *on probability* is equal to the probability that the load is zero and hence can be given as follows.

Corollary 3.2. *The active probability of the typical BS under the aforementioned approximation is*

$$p_{\rm on} = 1 - \mathbb{P}\left[\widetilde{S}_{\rm m} = 0\right]$$
$$= 1 - 2\pi \int_{r_{\rm t}=0}^{\infty} \mathbb{P}\left[S(r_{\rm t}) = 0\right] r_{\rm t} g_{|V_{\rm t}|}(\pi r_{\rm t}^2){\rm d}r_{\rm t},$$

with

$$\mathbb{P}\left[S(r_t) = 0\right] = \exp\left(-2\pi\lambda_{\rm L}\left(r - \int_0^r \frac{\exp\left(g\left(0, t\right)\right)t}{\sqrt{r^2 - t^2}}{\rm d}t\right)\right).$$

Further, the off probability $p_{\rm off} = 1 - p_{\rm on}$ denotes the probability that the typical BS stays silent.

B. SIR Coverage Probability

The SIR coverage probability is defined as the probability that SIR at the typical user is greater than a specific threshold τ. Since a silent BS does not cause interference at the typical vehicular user, coverage improves when the active probability $p_{\rm on}$ decreases. Using the machinery developed in this paper, the coverage probability for the typical vehicle can be derived as

$$\mathrm{p_c}(\tau) = \mathbb{P}[\mathtt{SIR} > \tau] = \frac{1}{1 + p_{\rm on}\int_1^{\infty}\frac{{\rm d}t}{1+t^{\alpha/2}\tau^{-1}}}. \quad (19)$$

Please refer to the extended version of this paper [1] for the complete proof. The purpose of just stating this result here is two fold: (i) it will help us provide useful insights in the next section, and (ii) it demonstrates the utility of the analytical framework developed in this paper. Further, the above result (19) is the same for both PTS and N-PTS. The active probability $p_{\rm on}$ for N-PTS is given in [16].

V. Numerical Results

In this section, we will first verify the accuracy of the PMF of $\widetilde{S}_{\rm m}$ by comparing it with the exact simulation results. The impact of vehicular density on the mean load of the typical BS will then be examined, followed by the verification of analytical CDF of k-th CD of PLP-MCP by simulation. We will also discuss the impact of various parameters such as BS density on the load distribution. Finally, we will discuss the impact of platooning on coverage probability. We use the following parameters in all our numerical results unless stated otherwise. The road density $\lambda_{\rm L} = 5/\pi$ km^{-1}, $\lambda_{\rm P} = 1$ platoons/km, and $a = 250$ m.

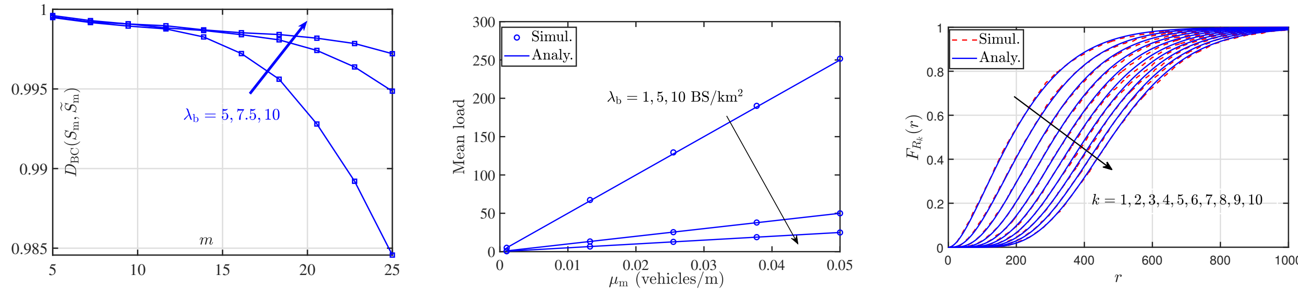

(a) (b) (c)

Fig. 1: (a) The BC $D_{\mathrm{BC}}(S_{\mathrm{m}}, \widetilde{S}_{\mathrm{m}})$ between the analytical (approximate) and simulated (exact) PMFs of the load on the typical BS. A value close to 1 implies that the PMF obtained using the approximation is close to the exact PMF. (b) Mean load as a function of vehicular density for three different values of BS density. We observe that increasing the BS density reduces the mean load on the typical BS. (c) The CDF of the CD for k-th ($k \in \{1, 2, 3, \ldots, 10\}$) nearest vehicles from the typical BS. For CDF of CD, $\lambda_{\mathrm{L}} = 5/\pi\ \mathrm{km}^{-1}$, $\lambda_{\mathrm{P}} = 1$ platoons/km, $a = 250$ m and $m = 3$.

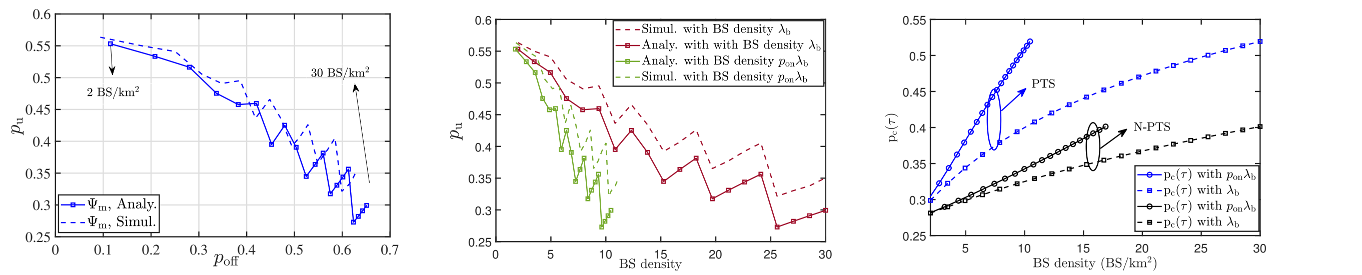

(a) (b) (c)

Fig. 2: (a) The plot of p_{u} versus p_{off} obtained by varying the BS density. The reduction in p_{u} denotes that the typical BS often serves more than the average load. (b) The plot of p_{u} as a function of BS density and the active BS density. An increase in BS density decreases p_{u} due to a drop in average load on the typical BS. In (a) and (b), the vehicular density is assumed to be $\mu = 15$ vehicles/km. (c) Coverage probability as a function of BS density. Here, the path loss exponent is $\alpha = 3.5$ and the SINR threshold is $\tau = 15$ dB.

A. Validation of PMF distribution of approximated load $\widetilde{S}_{\mathrm{m}}$ with the exact load S_{m}

To test the accuracy of the derived distributions of the approximate load $\widetilde{S}_{\mathrm{m}}$, we evaluate the Bhattacharyya coefficient (BC) [17] between the PMFs of the approximate load and the respective exact PMFs obtained using simulations. Note that for any two PMFs $p(\omega)$ and $q(\omega)$, the BC is defined as $D_{\mathrm{BC}}(p, q) = \sum \sqrt{p(x)q(x)}$. The BC $D_{\mathrm{BC}}(p, q)$, lies between 0 to 1, and a value close to 1 indicates good approximation. Fig. 1(a) shows the BC $\left(D_{\mathrm{BC}}(S_{\mathrm{m}}, \widetilde{S}_{\mathrm{m}})\right)$ for the typical BS load distribution for different values of m. From this result, we can observe that the approximation is remarkably close to the true result. The approximation improves further with decrease in platoon size m and increase in the BS density.

B. Mean load and the CD

In Fig. 1(b), we plot the analytical expression of the mean load along with its simulated values. We observe that the mean load on the typical BS increases as the vehicular density increases. Furthermore, this result is consistent with Corollary 3.1 that the mean load on the typical BS reduces with an increase in the BS density. Fig. 1(c) presents CDF of the k-th CD for Ψ_{m} validating analytical results with the simulation.

C. Variation of the load on the typical cell

To further understand the behavior of the typical BS's load, we will evaluate two additional metrics s_{avg} and p_{u}. The first metric s_{avg} is defined as the mean load of the typical BS when it is active, *i.e.*

$$s_{\mathrm{avg}} = \mathbb{E}\left[\widetilde{S}_{\mathrm{m}} | \widetilde{S}_{\mathrm{m}} > 0\right] = \mathbb{E}\left[\widetilde{S}_{\mathrm{m}}\right] / p_{\mathrm{on}}.$$

The second metric p_{u} denotes the probability that the load on the typical active BS is less than the s_{avg} *i.e.*

$$p_{\mathrm{u}} = \mathbb{P}\left[\widetilde{S}_{\mathrm{m}} \leq s_{\mathrm{avg}} | \widetilde{S}_{\mathrm{m}} > 0\right].$$

Note that p_{u} represents the fraction of time the system is in a very safe operational regime. In Fig. 2(a), we present the p_{u} as a function of p_{off} obtained by varying the BS density. As the BS density increases, the p_{off} value rises, indicating that the majority of BSs will be silent and therefore may not be serving any vehicles. Due to this reason, p_{u} drops and the active BSs are required to serve more than the average load. Consequently, while moving in a platoon, a serving BS must often carry a greater than average load. To further comprehend the behavior of p_{u} with active BS density, p_{u} is plotted as a function of both the BS density and the active BS density in Fig. 2(b). Increasing the BS density lowers the average load on the typical BS which consequently reduces the p_{u}. Further for a given value of p_{u}, the active BS density is significantly smaller than the net BS density.

D. Impact of platooning on the coverage probability

We present the SIR coverage probability with respect to the BS density for PTS in Fig. 2(c) along with the corresponding

N-PTS result from [16]. It is evident from this result that platoon movement of vehicles increases the coverage probability for the typical vehicle when compared to N-PTS. Note that the active probability $p_{\rm on}$ in PTS is less compared to N-PTS. As a consequence, less BSs do not interfere with the typical vehicular user, thereby resulting in an increased SIR at the user.

VI. Conclusion

In this paper, we have developed a comprehensive approach to the modeling and analysis of platooned vehicular traffic. The approach relies on a novel PP that captures vehicular platooning by explicitly capturing three layers of randomness: (i) irregular layout of the roads by modeling them as a PLP, (ii) randomness in the placement of the platoons on each road by modeling them as a PPP, and (iii) randomness in the location of each vehicle in a platoon by modeling them collectively as an MCP. After deriving several fundamental results for this *triply stochastic* process, which we called PLP-MCP, we focused explicitly on the V2I communication network for platooned traffic consisting of BSs that serve the platooned traffic. For this setting, we presented several key results related to the load distributions on the typical BS. We also discussed the impact of platooning on the SIR based coverage probability at the typical user.

Appendix

A. Proof of PGFL of $\Psi_{\rm m}$

The PGFL of $\Psi_{\rm m}$ is

$$G_{\Psi_{\rm m}}(v) = \mathbb{E}_{\Psi_{\rm m}}\left[\prod_{\mathbf{z}_{k,j,i}\in\Psi_{\rm m}} v(\mathbf{z}_{k,j,i})\right]$$
$$\stackrel{(a)}{=} \mathbb{E}_{\Phi_{\rm L}}\left[\prod\nolimits_{\ell_i\in\Phi_{\rm L}} \mathbb{E}_{\Psi_{\ell_i},\ell_i}\left[\prod\nolimits_{\mathbf{z}_{k,j}\in\Psi_{\ell_i},\ell_i} v(\mathbf{z}_{k,j})\right]\right]$$
$$\stackrel{(b)}{=} \mathbb{E}_{\Phi_{\rm L}}\left[\prod\nolimits_{\ell_i\in\Phi_{\rm L}} G_{\Psi_{\mathsf{L}(\rho_{\ell_i},\phi_{\ell_i})},\mathsf{L}(\rho_{\ell_i},\phi_{\ell_i})}(v)\right],$$

where (a) is obtained conditioned on $\Phi_{\rm L}$, and (b) is obtained by applying the PGFL of 1D MCP located on a line ℓ_i. Finally, applying the PGFL of the PLP, we get the PGFL of $\Psi_{\rm m}$.

B. Distribution of $S(r)$: Proof of Theorem 2

The number of vehicles $S(r)$ inside ball $\mathsf{B}_2(\mathrm{o},r)$ is $S(r) = \sum_{\ell_i\in\Phi_{\rm L},\rho_{\ell_i}\in[-r,r]} N_{\ell_i}$. Recall that

$$N_{\ell_i} = \Psi_{\ell_i}(\mathsf{B}_2(\mathrm{o},r)),$$

denotes the number of vehicles on $\ell_i = \mathsf{L}(\rho_{\ell_i},\phi_{\ell_i})$ falling inside $\mathsf{B}_2(\mathrm{o},r)$. The condition indicates that the distance of the line ρ_{ℓ_i} from the origin needs to be inside the range $[-r,\,r]$ for that line to have at least one point inside $\mathsf{B}_2(\mathrm{o},r)$ [8]. Now, RVs $\{N_{\ell_1}, N_{\ell_2},\ldots\}$ are independent and identically distributed (iid), hence PGF of $S(r)$ is

$$\mathcal{P}_{S(r)}(s) = \mathbb{E}\left[\prod\nolimits_{\ell_i\in\Phi_{\rm L},\rho_{\ell_i}\in[-r,r]} \mathcal{P}_{N_{\ell_i}}(s,r)\right]$$
$$= \mathbb{E}\left[\prod\nolimits_{\ell_i\in\Phi_{\rm L},\rho_{\ell_i}\in[-r,r]} \exp\left(g\left(s,\sqrt{r^2-\rho_{\ell_i}^2}\right)\right)\right],$$

where the PGF of N_{ℓ_i} is given by (8). Since $\rho_{\ell_i},\phi_{\ell_i}$ are points of a PPP in $\mathbf{C}^*$, using PGFL of PPP [12], we get the desired result. To get probability $\mathbb{P}[S(r)=k]$, we require the k-th derivative of PGF. If we define

$$f_{\rm m}(s,r) = 2\pi\lambda_{\rm L}\int_0^r \left(\exp(g(s,\sqrt{r^2-\rho^2}))-1\right)\mathrm{d}\rho.$$

the PGF $\mathcal{P}_{S(r)}(s)$ takes the form of $\exp(f_{\rm m}(s,r))$. Hence, we use the Faà di Bruno's formula [15] to get (14). To get k-th derivative $f_{\rm m}^{(k)}(r)$ of $f_{\rm m}(s,r)$ at $s=0$, we need to apply the Faà di Bruno's formula one more time to get (15).

References

[1] K. Pandey, K. R. Perumalla, A. K. Gupta, and H. S. Dhillon, "Fundamentals of vehicular communication networks with vehicle platoons," submitted to *IEEE Trans. Wireless Commun., available online: arXiv:2206.13277.*, 2022.

[2] S. Zeadally, M. A. Javed, and E. B. Hamida, "Vehicular communications for ITS: Standardization and challenges," *IEEE Commun. Standards Mag.*, vol. 4, no. 1, pp. 11–17, 2020.

[3] C. Perfecto, J. Del Ser, and M. Bennis, "Millimeter-wave V2V communications: Distributed association and beam alignment," *IEEE J. Sel. Areas Commun.*, vol. 35, no. 9, pp. 2148–2162, 2017.

[4] F. Baccelli and S. Zuyev, "Stochastic geometry models of mobile communication networks," in *Frontiers in Queueing: Models and Applications in Science and Engineering*. CRC Press, 1996, pp. 227–243.

[5] C.-S. Choi and F. Baccelli, "Poisson Cox point processes for vehicular networks," *IEEE Trans. Veh. Technol*, vol. 67, no. 10, pp. 10 160–10 165, 2018.

[6] ——, "An analytical framework for coverage in cellular networks leveraging vehicles," *IEEE Trans. on Commun.*, vol. 66, no. 10, pp. 4950–4964, 2018.

[7] H. S. Dhillon and V. V. Chetlur, *Poisson Line Cox Process: Foundations and Applications to Vehicular Networks*. Morgan & Claypool Publishers, 2020.

[8] V. V. Chetlur and H. S. Dhillon, "Coverage analysis of a vehicular network modeled as Cox process driven by Poisson line process," *IEEE Trans. Wireless Commun.*, vol. 17, no. 7, pp. 4401–4416, 2018.

[9] ——, "On the load distribution of vehicular users modeled by a Poisson line Cox process," *IEEE Wireless Commun. Lett.*, vol. 9, no. 12, pp. 2121–2125, 2020.

[10] C. Shao, S. Leng, Y. Zhang, A. Vinel, and M. Jonsson, "Performance analysis of connectivity probability and connectivity-aware MAC protocol design for platoon-based VANETs," *IEEE Trans. Veh. Technol*, vol. 64, no. 12, pp. 5596–5609, 2015.

[11] W. Yi, Y. Liu, Y. Deng, A. Nallanathan, and R. W. Heath, "Modeling and analysis of MmWave V2X networks with vehicular platoon systems," *IEEE J. on Sel. Areas Commun.*, vol. 37, no. 12, pp. 2851–2866, 2019.

[12] J. G. Andrews, A. K. Gupta, A. Alammouri, and H. S. Dhillon, *An Introduction to Cellular Network Analysis using Stochastic Geometry*. Morgan Claypool (Springer).

[13] M. Tanemura, "Statistical distributions of Poisson Voronoi cells in two and three dimensions," *Forma*, vol. 18, no. 4, pp. 221–247, 2003.

[14] J.-S. Ferenc and Z. Néda, "On the size distribution of Poisson Voronoi cells," *Physica A: Statistical Mechanics and its Applications*, vol. 385, no. 2, pp. 518–526, 2007.

[15] W. P. Johnson, "The curious history of Faà di Bruno's formula," *The American Mathematical Monthly*, vol. 109, no. 3, pp. 217–234, 2002.

[16] K. Pandey, K. R. Perumalla, A. K. Gupta, and H. S. Dhillon, "Load distribution in the typical and zero cells in a PLP-PPP vehicular communication network." [Online]. Available: https://home.iitk.ac.in/%7egkrabhi/subs/plpppp

[17] A. Bhattacharyya, "On a measure of divergence between two multinomial populations," *Sankhyā: the Indian Journal of Statistics*, pp. 401–406, 1946.